

Design of Robust H_∞ Combined with PID Controller Using Fuzzy Logic for a Missile Autopilot

N. T. Chung and C. H. Tinh*

Le Quy Don Technical University, Hanoi, Vietnam

The manuscript was received on 21 July 2023 and was accepted after revision for publication as research paper on 15 March 2024.

Abstract:

This paper presents the synthesis results of a robust H_∞ (H -infinity) loop-shaping controller combined with a PID (Proportional-Integral-Derivative) controller using fuzzy logic for the pitch autopilot of a tail control missile. The results take into consideration the change of mass, moment of inertia, and aerodynamic coefficients. The combination of the control signal of the robust controller and the PID controller is formed on the basis of adjusting the membership function of fuzzy logic according to the ITAE (Integral of Time-multiplied Absolute value of Error) optimization criterion. The performance and robustness of the missile autopilot are verified by nonlinear simulation.

Keywords:

missile autopilot, robust H_∞ loop-shaping control, PID control, fuzzy logic system, ITAE criterion

1 Introduction

In a missile autopilot system, the missile is a plant with many variable and uncertain parameters such as aerodynamic coefficients, mass, velocity, and moment of inertia. Unpredictable changes of parameters make it difficult to synthesize the controller. Many studies have been published dealing with the robust stability of a missile autopilot with uncertain parameters by applying several different control theories. To design a missile autopilot [1], for instance, the method of applying the pole-placement approach was used. To design the autopilot system to solve the problem of mass change during the motion of the missile [2], another approach was applied – the method of using the linear inequalities matrix combined with the gain-scheduling technique. The LPV-based (linear parameter varying) method was applied to the adaptive controller design for the pitch-axis autopilot [3], or the dynamic inverse method was also applied

* Corresponding author: Department of Aerospace Control Systems, Le Quy Don Technical University (LQDTU), Hanoi, Vietnam. E-mail: caohuutinh@lqdtu.edu.vn. ORCID: 0000-0001-8593-685X.

to design a nonlinear controller to guarantee the robustness of the missile [4]. In [5], the authors designed the autopilot for missiles with uncertain parameters by the back-stepping method; the results ensured stability and, at the same time, the performance of tracking. Recently, H_∞ synthesis methods have been used to design controllers for objects with many uncertainties [6]. These controllers were widely used in missile control, as they allow to ensure robustness and performance requirements in the presence of uncertainties and disturbances. In [7], a dynamic inversion controller was used for the inner loop and an H_∞ controller was used for the outer loop to achieve robust performance. In [8], Mohamed et al. proposed an autopilot design for an air-to-air guided missile based on H_∞ robust control to avoid noise and disturbance. However, an H_∞ controller has some disadvantages that need to be considered, such as high order or poor control performance. Moreover, the controller does not meet the performance requirements when the parameter changes over a wide range.

To improve control performance, researchers have combined different control methods. In particular, the method of combining the LQR controller with the PI controller yielded a higher performance in tracking than using only one LQR controller [9]. The combination of a PID controller and an H_∞ controller improves the ability to eliminate disturbances and increase stability [10]. In [11], the author proposed to combine the LQR controller with the H_∞ controller, and the results show that the combined controller can achieve the desired response time criteria with parameter uncertainties by automatic tuning and optimization of LQR weighted matrices. The combination of a PID controller and a LQR controller together with a fuzzy logic-based switching system takes advantage of both controllers and results in each controller maintaining the stability of the control system [12]. An optimized Takagi-Sugeno fuzzy mixed H_2/H_∞ robust controller was applied to suppress oscillation. It achieves better performance in terms of overshoot, transient time, and avoiding traps at a local optimal solution [13]. The controller designed by combining H_∞ control and fuzzy control achieves better performance for coupled-nonlinear systems than applying only one control method [14]. Thus, the combination of different control methods has improved control performance compared to using only one control method.

Following the approach of combining controllers using fuzzy logic, this paper presents the results of synthesizing a robust controller for the autopilot of the missile. The structure of the paper is as follows: After the introduction, the nonlinear dynamics model of the missile in the pitch plane is presented. The next section shows the results of using the H_∞ loop-shaping technique, PID control, and fuzzy logic to design a combined controller for a pitch missile autopilot. The performance of the autopilot is validated by nonlinear simulation in the MATLAB environment. The last section is the conclusion.

2 Missile Dynamics

Considering the typical aerodynamic missile, there are two pairs of wings that are symmetrical about the longitudinal axis. It is assumed that the missile is controlled stably around the longitudinal axis and that there is no coupling between the control planes. The rotation of the missile in the pitch plane is represented in Eq. (1) [15]:

$$\begin{aligned}\dot{\alpha} &= \frac{q_{\infty} S_{\text{ref}}}{m V_M} (\sin \alpha C_A - \cos \alpha C_N) + q - \sin \alpha \frac{q_{\infty} S_{\text{ref}} C_T}{m V_M} \\ \dot{q} &= \frac{q_{\infty} S_{\text{ref}} d}{I_y^b} (C_m + \bar{s} C_N)\end{aligned}\quad (1)$$

where α is the angle of attack; q is the angular speed of the missile; q_M is the dynamic pressure; S_{ref} is the aerodynamic reference area of the missile; m is the mass of the missile; V_M is the missile's speed; d is the diameter of the missile; \bar{s} is the converted distance (in missile diameter) from the center of gravity of the missile to the center of pressure; I_y^b is the pitch moment of inertia of the missile; C_A , C_N , C_T , and C_m are the axial force coefficient, the normal force coefficient, the thrust coefficient, and the pitch moment coefficient at moment reference center, respectively. C_A , C_N , and C_m are approximated by expressions (2), (3), and (4):

$$C_N = C_{N\alpha}\alpha + C_{N\alpha|\alpha}|\alpha| + C_{N\alpha^3}\alpha^3 + (C_{N\delta_q} + C_{N\alpha\delta_q}\alpha)\delta_q + (C_{Nq}q + C_{N\dot{\alpha}}\dot{\alpha})\frac{d}{2V_M} \quad (2)$$

$$C_m = C_{m\alpha}\alpha + C_{m\alpha|\alpha}|\alpha| + C_{m\alpha^3}\alpha^3 + C_{m\delta_q}(\alpha)\delta_q + (C_{mq}q + C_{m\dot{\alpha}}\dot{\alpha})\frac{d}{2V_M} \quad (3)$$

$$\begin{aligned}C_A &= C_{A_0} + C_{A|\alpha}|\alpha| + C_{A\alpha^2}\alpha^2 + C_{A|\alpha^3}|\alpha|^3 + \Delta C_{Ab} + \\ &+ (C_{A\delta_q} \text{sgn } \delta_q + C_{A\alpha\delta_q}\alpha + C_{A\alpha^2\delta_q}\alpha^2)\delta_q\end{aligned}\quad (4)$$

The aerodynamic coefficients (2), (3), (4) are substituted into Eq. (1), we have:

$$\begin{cases} \dot{\alpha} = a_{11}^a \alpha + a_{12}^a q + b_{11}^a \delta_q \\ \dot{q} = a_{21}^a \alpha + a_{22}^a q + b_{22}^a \delta_q \end{cases} \quad (5)$$

where

$$\begin{aligned}a_{11}^a &= \frac{q_{\infty} S_{\text{ref}}}{m V_M D_{\dot{\alpha}}} \left[\sin \alpha (C_{A\alpha} + C_{A\alpha^2}|\alpha| + C_{A\alpha^3}\alpha^2) \text{sgn } \alpha + \text{sinc } \alpha (C_{A_0} + \Delta C_{Ab} - C_T) \right. \\ &\quad \left. - \cos \alpha (C_{N\alpha} + C_{N\alpha|\alpha}|\alpha| + C_{N\alpha^3}\alpha^2) \right]\end{aligned}$$

$$\text{sinc } \alpha = \begin{cases} \frac{\sin \alpha}{\alpha}, & \alpha \neq 0 \\ 1, & \alpha = 0 \end{cases}$$

$$a_{12}^a = \frac{1}{D_{\dot{\alpha}}} \left(1 - \frac{q_{\infty} S_{\text{ref}} d}{2m V_M^2} \cos \alpha C_{Nq} \right)$$

$$a_{21}^a = \frac{q_{\infty} S_{\text{ref}} d}{I_y^b} \left[C_{m\alpha} + C_{m\alpha|\alpha}|\alpha| + C_{m\alpha^3}\alpha^2 + \bar{s} (C_{N\alpha} + C_{N\alpha|\alpha}|\alpha| + C_{N\alpha^3}\alpha^2) \right]$$

$$\begin{aligned}
a_{22}^a &= \frac{q_\infty S_{\text{ref}} d^2}{2V_M I_y^b} (C_{m\dot{q}} + \bar{s} C_{Nq}) \\
b_{11}^a &= \frac{q_\infty S_{\text{ref}}}{mV_M D_{\dot{\alpha}}} \left[(\sin \alpha C_{A\delta_q} \text{sgn } \delta_q - \cos \alpha C_{N\delta_q}) + \alpha (\sin \alpha C_{A\alpha\delta_q} - \cos \alpha C_{N\alpha\delta_q}) + \sin \alpha C_{A\alpha^2\delta_q} \alpha^2 \right] \\
b_{21}^a &= \frac{q_\infty S_{\text{ref}} d}{I_y^b} \left[C_{m\delta_q} \alpha + \bar{s} (C_{N\delta_q} + \alpha C_{N\alpha\delta_q}) \right] \\
D_{\dot{\alpha}} &= 1 + \frac{q_\infty S_{\text{ref}}}{mV_M} \cos \alpha \frac{d}{2V_M} C_{N\dot{\alpha}} \\
C_{m\delta_q}(\alpha) &= \begin{cases} C_{m\alpha\delta_q}^0 + \sum_{j=1}^4 C_{m\alpha\delta_q}^j (\alpha)^j & \alpha \geq 0 \\ 2C_{m\alpha\delta_q}^0 - \sum_{j=1}^4 C_{m\alpha\delta_q}^j (|\alpha|)^j & \alpha < 0 \end{cases}
\end{aligned}$$

where δ_q is the control fin deflection in pitch; $\text{sgn}(\cdot)$ is the sign function.

Writing Eq. (5) in matrix form, we have

$$\begin{bmatrix} \dot{\alpha} \\ \dot{q} \end{bmatrix} = \begin{bmatrix} a_{11}^a & a_{12}^a \\ a_{21}^a & a_{22}^a \end{bmatrix} \begin{bmatrix} \alpha \\ q \end{bmatrix} + \begin{bmatrix} b_{11}^a \\ b_{21}^a \end{bmatrix} \delta_q \quad (6)$$

The normal acceleration of the missile is presented in Eq. (7):

$$n_y = -\frac{1}{m} q_\infty S_{\text{ref}} C_N \quad (7)$$

Let

$$\left. \begin{aligned} \mathbf{x} &= [\alpha \quad q]^T \\ \mathbf{u} &= \delta_q \\ \mathbf{y} &= [n_y \quad \alpha \quad q]^T \end{aligned} \right\}$$

$$\mathbf{A}_a = \begin{bmatrix} a_{11}^a & a_{12}^a \\ a_{21}^a & a_{22}^a \end{bmatrix}; \quad \mathbf{B}_a = \begin{bmatrix} b_{11}^a \\ b_{21}^a \end{bmatrix}; \quad \mathbf{C}_a = \begin{bmatrix} c_{11} & c_{12} \\ 1 & 0 \\ 0 & 1 \end{bmatrix}; \quad \mathbf{D}_a = \begin{bmatrix} d_{11} \\ 0 \\ 0 \end{bmatrix}$$

where

$$\begin{aligned}
c_{11} &= -\frac{1}{m} q_\infty S_{\text{ref}} \left(C_{N\alpha} + C_{N\alpha|\alpha|} |\alpha| + C_{N\alpha^3} \alpha^2 + C_{N\dot{\alpha}} \frac{d}{2V_M} a_{11}^a \right) \\
c_{12} &= -\frac{1}{m} q_\infty S_{\text{ref}} (C_{Nq} + C_{N\dot{\alpha}} a_{12}^a) \frac{d}{2V_M} \\
d_{11} &= -\frac{1}{m} q_\infty S_{\text{ref}} \left[(C_{N\delta_q} + C_{N\alpha\delta_q} \alpha) + C_{N\dot{\alpha}} \frac{d}{2V_M} b_{11}^a \right]
\end{aligned}$$

Then, the missile dynamics model in the pitch plane is expressed in the form of state space as follows Eq. (8):

$$\begin{cases} \dot{\mathbf{x}} = \mathbf{A}_a \mathbf{x} + \mathbf{B}_a \mathbf{u} \\ \mathbf{y} = \mathbf{C}_a \mathbf{x} + \mathbf{D}_a \mathbf{u} \end{cases} \quad (8)$$

3 Synthesis of Controller and Evaluation

3.1 Uncertain Model of the Missile

Without considering the dynamics of sensors and assuming that the angle of attack, angular speed, and normal acceleration are measured. The structure diagram of the missile autopilot with a robust H_∞ controller is shown in Fig. 1, where n_{yc} and n_y are the normal acceleration command and normal acceleration output respectively; δ_{qc} and δ are the input and output of the actuator respectively; δ_q is the control fin deflection limited by a saturation model.

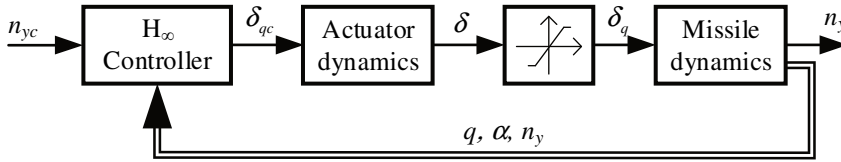


Fig. 1 Diagram of the missile autopilot

Actuator dynamics is approximated as a second-order system as follows (9):

$$\begin{bmatrix} \dot{\delta} \\ \ddot{\delta} \end{bmatrix} = \begin{bmatrix} 0 & 1 \\ -\omega_a^2 & -2\zeta_a \omega_a \end{bmatrix} \begin{bmatrix} \delta \\ \dot{\delta} \end{bmatrix} + \begin{bmatrix} 0 \\ \omega_a^2 \end{bmatrix} \delta_{qc} \quad (9)$$

where ζ_a and ω_a are the damping ratio and natural frequency of the actuator respectively. $\zeta_a = 0.707$; $\omega_a = 150$ rad/s.

Consider the typical aerodynamic missile model with geometrical parameters in Fig. 2, and aerodynamic coefficients in Tab. 1 [15]. The angle of attack is limited to $\pm 30^\circ$, and the rudder rotation is limited to $\pm 30^\circ$. The main parameters of the missile are shown in Tab. 2.

From Eq. (8), the uncertain model of the missile at the boundary values of the parameters of mass, moment of inertia, position of the center of gravity, angle of attack, and rudder rotation is calculated and expressed as follows:

$$\begin{cases} \dot{\mathbf{x}} = \begin{bmatrix} a_{11}^{unc} & 0.9995 \\ a_{21}^{unc} & -9.3868 \end{bmatrix} \mathbf{x} + \begin{bmatrix} b_{11}^{unc} \\ b_{21}^{unc} \end{bmatrix} \mathbf{u} \\ \mathbf{y} = \begin{bmatrix} c_{11}^{unc} & 0.005 \\ 1 & 0 \\ 0 & 1 \end{bmatrix} \mathbf{x} + \begin{bmatrix} d_{11}^{unc} \\ 0 \\ 0 \end{bmatrix} \mathbf{u} \end{cases} \quad (10)$$

where

$$a_{11}^{unc} \in [-4.2706, -2.4625]; \quad a_{21}^{unc} \in [-2660.5, -527.47]$$

$$b_{11}^{unc} \in [-0.6319, 0.0224]; \quad b_{21}^{unc} \in [-4242.3, -2135.4]$$

$$c_{11}^{unc} \in [-38.1756, -18.7101]; \quad d_{11}^{unc} \in [-5.9507, -4.1760]$$

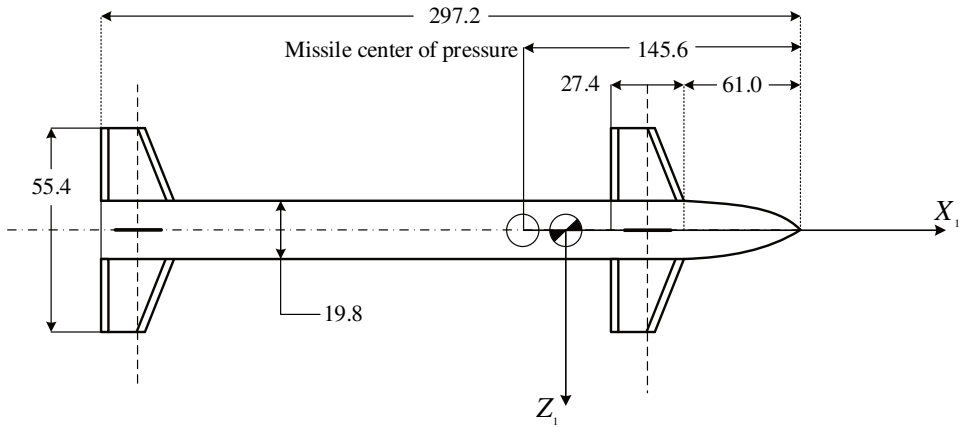


Fig. 2 Missile model

Tab. 1. Aerodynamic coefficients of the missile

Coefficient	Value	Coefficient	Value	Coefficient	Value
$C_{N\alpha}$	$2.020 \cdot 10^{-1}$	$C_{m\alpha}$	$1.373 \cdot 10^{-1}$	$C_{A\alpha^2}$	$-7.642 \cdot 10^{-5}$
$C_{N\alpha \alpha }$	$1.110 \cdot 10^{-2}$	$C_{m\alpha \alpha }$	$-1.020 \cdot 10^{-2}$	$C_{A\alpha^3}$	$2.111 \cdot 10^{-6}$
$C_{N\alpha^3}$	$-1.131 \cdot 10^{-5}$	$C_{m\alpha^3}$	$-6.864 \cdot 10^{-5}$	ΔC_{Ab}	$1.062 \cdot 10^{-1}$
$C_{N\delta_q}$	$6.961 \cdot 10^{-2}$	C_{mq}	$-1.8560 \cdot 10^{-1}$	$C_{A\delta_q}$	$-2.282 \cdot 10^{-2}$
$C_{N\alpha\delta_q}$	$4.066 \cdot 10^{-4}$	$C_{m\dot{\alpha}}$	-1.405	$C_{A\alpha\delta_q}$	$1.904 \cdot 10^{-3}$
C_{Nq}	$5.734 \cdot 10^{-1}$	C_{A_0}	$4.362 \cdot 10^{-1}$	$C_{A\alpha^2\delta_q}$	$-2.708 \cdot 10^{-5}$
$C_{N\dot{\alpha}}$	$-2.781 \cdot 10^{-1}$	$C_{A\alpha}$	$3.886 \cdot 10^{-3}$		

Tab. 2. Main parameters of the missile

Parameter	Units	Value	Parameter	Units	Value
Altitude	m	6 000	Speed	M	2.50
Position mass center, end of boost (from nose)	cm	143.6	Missile mass, launch	kg	101.30
Position mass center, burnout (from nose)	cm	128.8	Missile mass, burn out	kg	87.27
Body frontal area	dm ²	3.0828	Pitch moment of inertia, launch	kg·m ²	33.20
Burning time, sustain engine	s	8	Pitch moment of inertia, burnt out	kg·m ²	32.00

The step responses of several samples of the uncertain model of the missile are shown in Fig. 3. The orange line is the step response of the nominal model, and the rest are the step responses of the model with random values of the uncertain parameters.

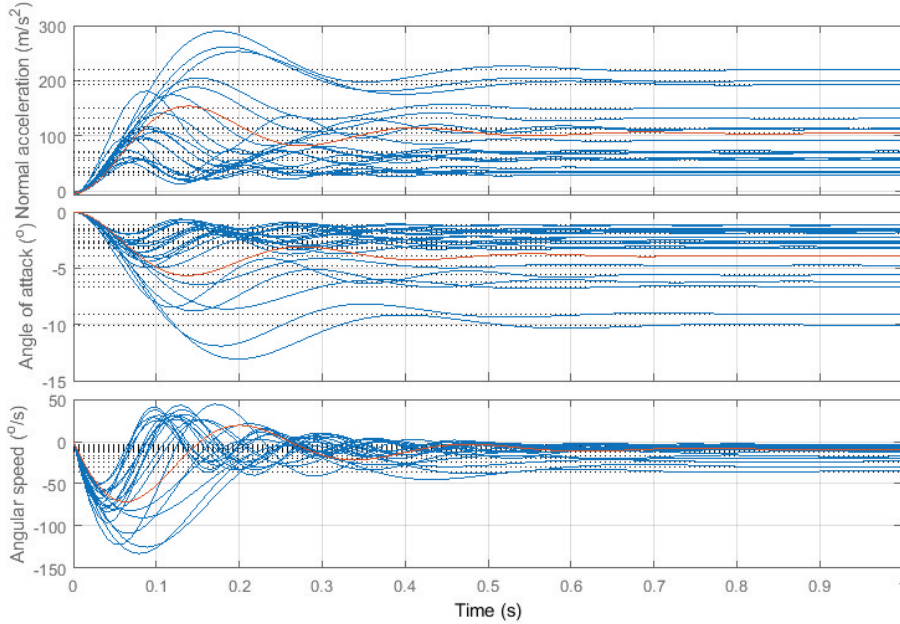


Fig. 3 Step response of the uncertain model of the missile

3.2 Synthesis of Robust H_∞ Loop-Shaping Controller

A control system is robust if it remains stable and meets certain performance criteria under the influence of uncertainties. The task of robust control synthesis is to find such a controller for a given system that the closed system is robust. The H_∞ optimization method has been proven to be a robust and efficient design method for time-invariant, linear control systems. Although it is an efficient method, the perturbation representations of the model are limited by the number of poles to the right of the complex plane. In addition, unwanted cancellation of poles and zeros can occur between the nominal model and the H_∞ controller [16]. To design a robust controller, the H_∞ loop-shaping control technique is an efficient method, whereby the restrictions on the number of poles on the right of the complex plane can be extended without producing cancellation of pole and zero points between the nominal model and the designed controller. In addition, this method does not require an iterative procedure to obtain an optimal controller and thus improves computational efficiency. Therefore, this paper uses the H_∞ loop-shaping design method.

Suppose the plant contains uncertain components, which are represented by Eq. (11):

$$G_\Delta = (N_S + \Delta_{NS})(M_S + \Delta_{MS})^{-1} \quad (11)$$

where N_S and M_S are the numerator and denominator of the nominal transfer function G_0 of the plant, respectively; Δ_{NS} and Δ_{MS} are the uncertain components of the numerator and denominator, respectively. $\|\Delta_{NS}, \Delta_{MS}\|_\infty \leq \varepsilon$, where ε is the stability margin ($\varepsilon > 0$).

In Fig. 4, the designed elements in the structure diagram of the controller are weight functions W_1 (pre-compensator) and W_2 (post-compensator). They are combined with the nominal plant G_0 to achieve the shaped plant G_S . As a result, the shaped plant can be written as follows:

$$G_S = W_2 G_0 W_1. \quad (12)$$

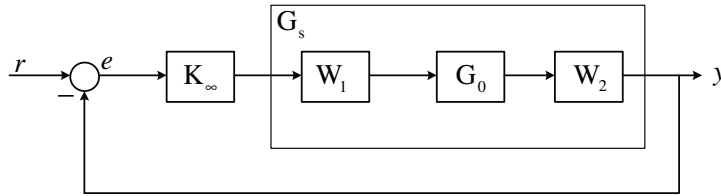


Fig. 4 Structure diagram of the H_∞ loop-shaping controller

Then, the controller K_∞ is synthesized for the plant G_S by solving the inequality Eq. (13):

$$\left\| \begin{array}{l} (I + G_S K_\infty)^{-1} M_S^{-1} \\ K_\infty (I + G_S K_\infty)^{-1} M_S^{-1} \end{array} \right\|_\infty \leq \varepsilon^{-1} \quad (13)$$

The H_∞ loop-shaping feedback controller is:

$$K = W_1 K_\infty W_2 \quad (14)$$

Using the `loopsyn()` and `balred()` functions in MATLAB to synthesize and reduce the order of the H_∞ loop-shaping controller for the uncertain plant (10), we get the parameters of the controllers corresponding to feedback loops according to angular speed, angle of attack, and normal acceleration as follows:

$$\begin{aligned} K_{H \text{ inf } q} &= \frac{-28044 - 3899.3s - 119.3225s^2 - 6.05s^3 - 0.0368s^4}{251760s + 147030s^2 + 11493s^3 + s^4} \\ K_{H \text{ inf } a} &= \frac{1497.7 + 6287.3s + 981.3252s^2}{87s + s^2} \\ K_{H \text{ inf } n} &= \frac{-1509.3 - 111.5642s - 0.5655s^2}{745.7079s + s^2} \end{aligned} \quad (15)$$

Fig. 5 presents the investigation results of the autopilot, which has the H_∞ loop-shaping controller Eq. (15). The input is the normal acceleration command, and the missile model is nonlinear. The result shows that, when the command has a suitable value, the normal acceleration of the missile tracks the command with good performance, ensuring a small steady-state error and a short transient time. However, when the input is small (the normal acceleration command $n_{yc} = 1$), the control performance is significantly reduced, even unstable. This disadvantage is solved by the PID controller below.

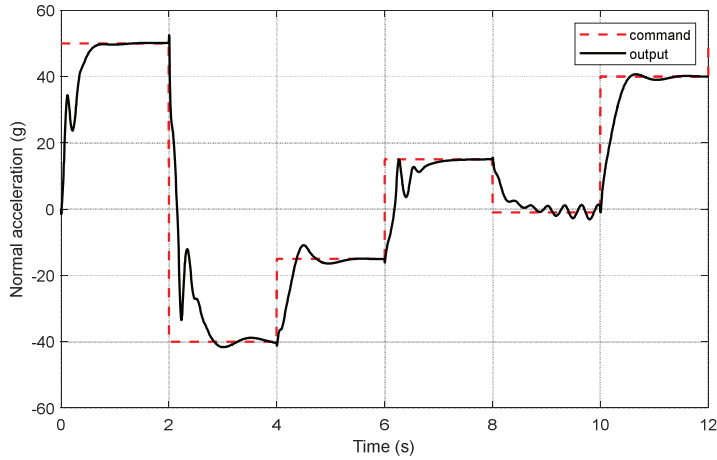


Fig. 5 Normal acceleration of missile with H_∞ loop-shaping controller

3.3 Synthesis of PID Controller

The conventional PID controller has a simple structure. It can simultaneously improve both the response time and the steady-state error of the control system within a certain range. Therefore, with the aim of supplementing the H_∞ loop-shaping controller in the case of a small input, the article proceeds to synthesize a PID controller.

A continuous-time PID controller calculates the control signal $u(t)$ based on the error $e(t)$ as follows (16):

$$u(t) = K_P e(t) + K_I \int_0^t e(t) dt + K_D \frac{de(t)}{dt} \tag{16}$$

where the parameters of the controller are K_P (proportional gain), K_I (integration gain), and K_D (derivative gain).

Fig. 6 shows the diagram of an autopilot with a PID controller in the outer loop and an H_∞ loop-shaping controller in the inner loop. The input to the system is the normal acceleration command.

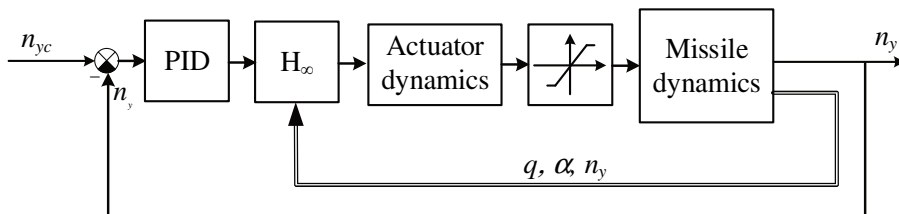


Fig. 6 The diagram of autopilot with PID controller in the outer loop, H_∞ loop-shaping controller in the inner loop

Using the Simulink Design Optimization toolbox, the PID controller parameters after turning are as follows: $K_P = 3.1080$, $K_I = 15.9340$, and $K_D = 0.1187$.

In Fig. 7, the result shows that the PID controller significantly improves the control performance of the system when the input signal is small. However, when the

input signal is large, the quality of the system decreases compared to the quality of the system without the PID controller (see the results in Section 3.2).

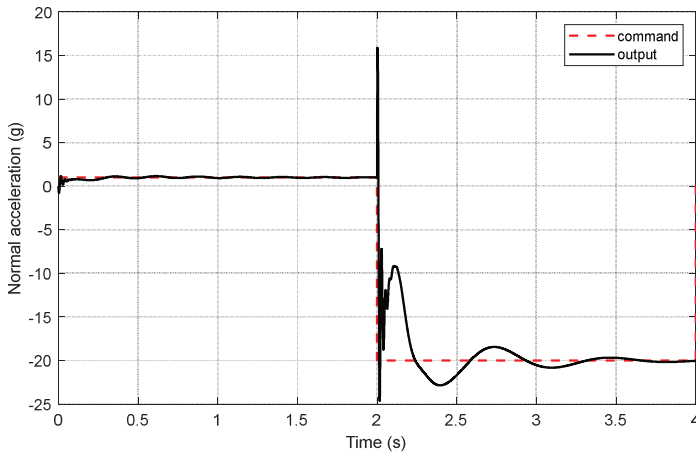


Fig. 7 Normal acceleration of missile with PID and H_∞ loop-shaping controllers

3.4 Combination of H_∞ Loop-Shaping Controller and PID Controller Using Fuzzy Logic System

The advantages and disadvantages of the H_∞ loop-shaping controller and the PID controller presented in sections 3.2 and 3.3 lead to the idea of combining these two controllers. This paper chooses the combining mechanism using a fuzzy logic system.

The architecture of a fuzzy logic system is shown in Fig. 8 [17]. In general, a fuzzy logic system establishes the specifics of the nonlinear mapping of an input data vector into a scalar output based on fuzzy set theory and fuzzy logic. It includes four parts: the fuzzifier, rules, inference engine, and defuzzifier. The fuzzifier component transforms raw inputs into fuzzy sets using linguistic terms and membership functions. The rules part contains the rules and membership functions that regulate decisions in the fuzzy logic system. The inference engine is a tool that maps fuzzy input sets into fuzzy output sets. The defuzzifier maps fuzzy output sets into explicit outputs. This is the output stage of a fuzzy logic system.

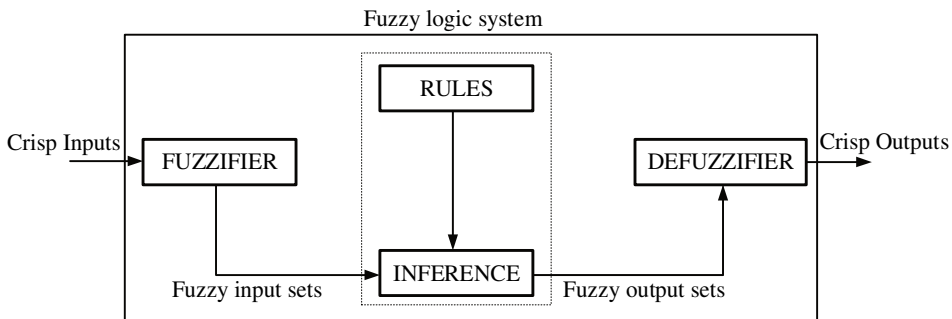


Fig. 8 Architecture of a fuzzy logic system

Fig. 9 is the diagram of the missile autopilot with a fuzzy logic system. The mechanism of combining the two controllers is designed in such a way that when the input (n_{yc}) is large, the H_∞ loop-shaping controller is used. When the input is small and the error $e(t)$ is small, the PID controller is used. This combination mechanism brings into play the advantages of both the H_∞ loop-shaping controller and the PID controller.

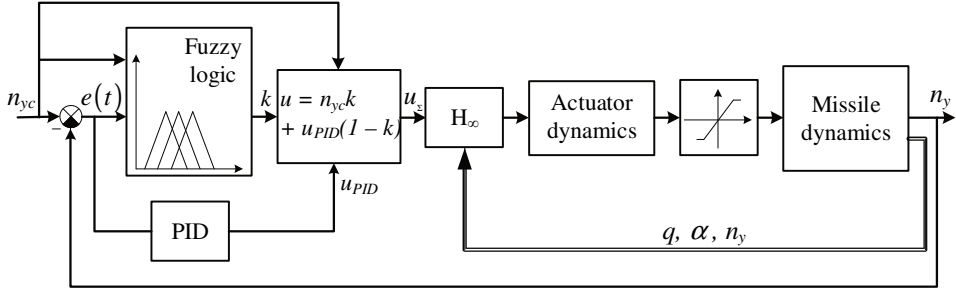


Fig. 9 Missile autopilot with combining two controllers

By using the error signal and the input command, the fuzzy logic system calculates the factor k ($0 \leq k \leq 1$), which is then used to calculate the control instruction by combining the signals of the H_∞ loop-shaping controller and the PID controller.

$$u_\Sigma = n_{yc} \cdot k + u_{PID} \cdot (1 - k) \tag{17}$$

The membership functions of the fuzzy logic system are shown in Fig. 10. The fuzzy rules are simply set up as follows:

- IF (n_{yc} is small) AND ($e(t)$ is small) THEN (k is small),
- IF (n_{yc} is big) THEN (k is big).

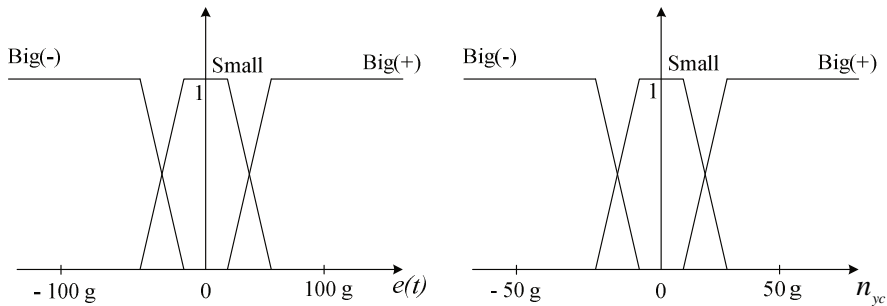


Fig. 10 Membership functions

The membership functions are adjusted to minimize the quality cost function according to the ITAE criterion:

$$J_{\min} = \int_0^{\infty} t \cdot |e(t)| dt \rightarrow \min$$

Simulation results when combining the H_∞ loop-shaping controller and the PID controller with a fuzzy logic system are shown in Fig. 11. The results show that, when using the fuzzy logic matching mechanism, the system performance is better than

when using the H_∞ loop-shaping or PID controller alone. Thus, the combined controller has solved the requirements of the autopilot when considering the nonlinearity of the missile dynamics model along with the change of parameters in the wide range, while maintaining control performance. First, when the command is small, the system with the combined controller is stable and has good tracking (during the period from the 8th to the 10th second). Second, when the command is large, the system has good performance (from initialization to the 4th second).

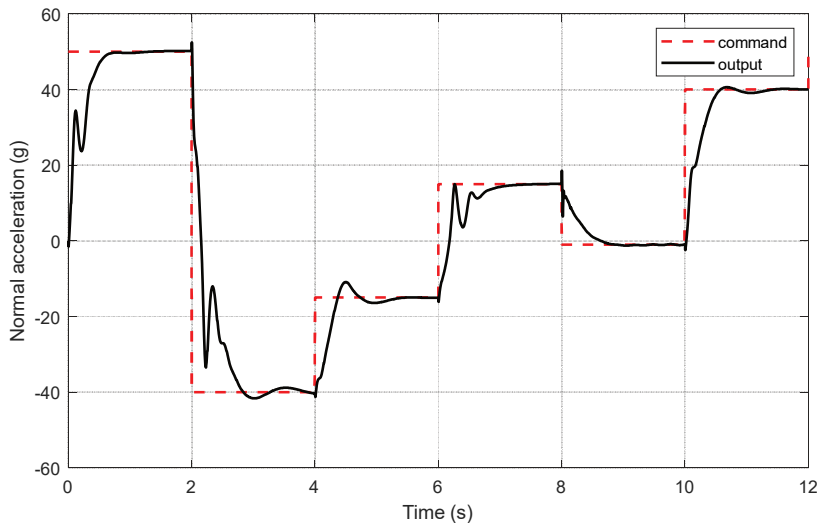


Fig. 11 Normal acceleration of missile with combination controller

4 Conclusion

This paper presents the results of a synthesis study of a robust H_∞ loop-shaping controller combined with a PID controller using a fuzzy logic system for the pitch autopilot of a missile with variable parameters. The control signals of the two controllers are combined by a fuzzy logic system according to the minimization of the ITAE criterion. The results of nonlinear simulation in the MATLAB/Simulink environment confirmed that the controller has good performance and is stable with respect to changes in parameters. Additionally, the components of the controller are not too complicated to compute.

References

- [1] RYU, S.M., D.Y. WON, C.H. LEE and M.J. TAHK. Missile Autopilot Design for Agile Turn Control During Boost-phase. *International Journal of Aeronautical and Space Sciences*, 2011, **12**(4), pp. 365-370. DOI 10.5139/IJASS.2011.12.4.365.
- [2] WON, D.Y., M.J. TAHK and K.Y. KIM. Robust Gain-scheduling Technique for an Agile Missile Subject to Mass Variation. In: *International Conference on Control, Automation and Systems (ICCAS)*. Gyeonggi-do: IEEE, 2010, pp.2119-2123. DOI 10.1109/ICCAS.2010.5670191.

-
- [3] THEODOULIS, S. and G. DUC. Missile Autopilot Design: Gain Scheduling and the Gap Metric. *Journal of Guidance, Control, and Dynamics*, 2009, **32**(3). DOI 10.2514/1.34756.
- [4] ZHONG, L., B. CAO, X. LIANG and X. JIA. A Composite Dynamic Inverse Controller Design for Agile Missile. In: *6th World Congress on Intelligent Control and Automation*. Dalian: IEEE, 2006, pp. 930-933. DOI 10.1109/WCICA.2006.1712480.
- [5] LEE, S., Y. KIM, Y. LEE, G. MOON and B.E. JEON. Robust-Backstepping Missile Autopilot Design Considering Time-Varying Parameters and Uncertainty. *IEEE Transactions on Aerospace and Electronic Systems*, 2020, **56**(6), pp. 4269-4287. DOI 10.1109/TAES.2020.2990819.
- [6] DOYLE, J., K. GLOVER, P. KHARGONEKAR and B. FRANCIS. State-space Solutions to Standard H_2 and H_∞ Control Problems. In: *1988 American Control Conference*. Atlanta: IEEE, 1988, pp. 1691-1696. DOI 10.23919/ACC.1988.4789992.
- [7] SADRAEY, M. and R. COLGREN. Robust Nonlinear Controller Design for a Complete UAV Mission. In: *AIAA Guidance, Navigation, and Control Conference and Exhibit*. Keystone: AIAA, 2006, pp. 1-20. DOI 10.2514/6.2006-6687.
- [8] MOHAMED, A., G. EL-SHEIKH, A.N. OUDA and A.M. YOUSSEF. Robust Autopilot Design and Hardware-in-the-Loop for Air to Air Guided Missile. *Advances in Military Technology*, 2017, **12**(2), pp. 281-300. DOI 10.3849/aimt.01207.
- [9] ELKHATEM, A.S. and S.N. ENGIN. Robust LQR and LQR-PI Control Strategies Based on Adaptive Weighting Matrix Selection for a UAV Position and Attitude Tracking Control. *Alexandria Engineering Journal*, 2022, **61**(8), pp. 6275-6292. DOI 10.1016/j.aej.2021.11.057.
- [10] NAIR, S.S. and G.R. SANGEETHA. Hybrid PID/ H_∞ Control of Active Magnetic Bearings. *International Journal of Electrical Engineering*, 2011, **4**(1). ISSN 0974-2158.
- [11] HAZEM, I.A. Mixed LQR/H-Infinity Controller Design for Uncertain Multivariable Systems. *Emirates Journal for Engineering Research*, 2015, **20**(1), pp. 101-107. ISSN 1022-9892.
- [12] REZA, M.A., A. MAHDOUDI, E. POURABDOLLAH and G. KLANČAR. Combined PID and LQR Controller Using Optimized Fuzzy Rules. *Soft Computing*, 2019, **23**, pp. 5143-5155. DOI 10.1007/s00500-018-3180-3.
- [13] LISHENG, L., J. QIAN, Y. ZOU, D. TIAN, Y. ZENG, F. CAO and X. LI. Optimized Takagi-Sugeno Fuzzy Mixed H_2/H_∞ Robust Controller Design Based on CPSOGSA Optimization Algorithm for Hydraulic Turbine Governing System. *Energies*, 2022, **15**(13), 4771-4801. DOI 10.3390/en15134771.
- [14] MOHAMMED, Y.H., H.I. ALI and H.M. JASSIM. Hybrid H-Infinity Fuzzy Logic Controller Design. *Journal of Engineering Science and Technology*, 2020, **15**(1), pp. 1-21.
- [15] HERNÁNDEZ, F.D.B.I. *Optimization of the Integrated Guidance and Control for a Dual Aerodynamic Control Missile* [PhD Thesis]. Universidad Politécnica de Madrid, 2015. DOI 10.20868/UPM.thesis.38301.
- [16] SEFTON, J. and K. GLOVER. Pole/zero Cancellations in the General H_∞ Problem with Reference to a Two Block Design. *Systems & Control Letters*, 1990, **14**(4), pp. 295-306. DOI 10.1016/0167-6911(90)90050-5.
- [17] MENDEL, J.M. Fuzzy Logic Systems for Engineering: a Tutorial. *Proceedings of the IEEE*, 1995, **83**(3), pp. 345-377. DOI 10.1109/5.364485.